



## OPEN

## SUBJECT AREAS:

BIOGEOCHEMISTRY  
BIOOCEANOGRAPHY

Received

6 September 2013

Accepted

10 December 2013

Published

20 January 2014

Correspondence and  
requests for materials  
should be addressed to  
H.S.F. (hefi@pml.ac.  
uk)

# Fine-scale nutrient and carbonate system dynamics around cold-water coral reefs in the northeast Atlantic

Helen S. Findlay<sup>1</sup>, Sebastian J. Hennige<sup>2</sup>, Laura C. Wicks<sup>2</sup>, Juan Moreno Navas<sup>2</sup>,  
E. Malcolm S. Woodward<sup>1</sup> & J. Murray Roberts<sup>2,3,4</sup>

<sup>1</sup>Plymouth Marine Laboratory, Prospect Place, West Hoe, Plymouth, England, PL1 3DH, UK, <sup>2</sup>Centre for Marine Biodiversity & Biotechnology, School of Life Sciences, Heriot-Watt University, Edinburgh, Scotland, EH14 4AS, UK, <sup>3</sup>Scottish Association for Marine Science, Oban, PA37 1QA, UK, <sup>4</sup>Center for Marine Science, University of North Carolina, Wilmington, 601 S. College Road, Wilmington, North Carolina, 28403-5928, USA.

Ocean acidification has been suggested as a serious threat to the future existence of cold-water corals (CWC). However, there are few fine-scale temporal and spatial datasets of carbonate and nutrients conditions available for these reefs, which can provide a baseline definition of extant conditions. Here we provide observational data from four different sites in the northeast Atlantic that are known habitats for CWC. These habitats differ by depth and by the nature of the coral habitat. At depths where CWC are known to occur across these sites the dissolved inorganic carbon ranged from 2088 to 2186  $\mu\text{mol kg}^{-1}$ , alkalinity ranged from 2299 to 2346  $\mu\text{mol kg}^{-1}$ , and aragonite  $\Omega$  ranged from 1.35 to 2.44. At two sites fine-scale hydrodynamics caused increased variability in the carbonate and nutrient conditions over daily time-scales. The observed high level of variability must be taken into account when assessing CWC sensitivities to future environmental change.

**S**pecific dynamics such as temperature, salinity, oxygen availability, light, and water currents, have been shown to control reef and coral growth on tropical shallow-water zooxanthellate coral reefs [e.g.<sup>1,2</sup>], but also, more recently, on cold-water non-zooxanthellate coral reefs [e.g.<sup>3,4</sup>]. While the physical dynamics are clearly important, the biogeochemical dynamics (interlinked with the physics), such as the carbonate ion concentration or nutrients<sup>5</sup>, are also recognized to contribute to reef and coral growth. On tropical coral reefs, carbon and nutrient dynamics have been shown to be highly variably<sup>6–8</sup>, but the presence of the reefs themselves can also contribute to the variability in carbon and nutrients over daily and seasonal time-scales<sup>9–11</sup>.

Dullo *et al.*<sup>4</sup> suggested that cold-water coral (CWC) reefs are not randomly distributed but instead can be found at certain density ranges, specifically from 27.35 to 27.65. This density pre-requisite has been confirmed in more recent observations of both deep and shallow CWC reefs [e.g.<sup>12,13</sup>], however not all CWC habitats are found in such a narrow density range<sup>14</sup>, and it is highly relevant we consider all these types of habitats. While this identifier has been used to locate living CWC reefs, Dullo *et al.*<sup>4</sup> also highlight the need for further research on related processes including nutrient inventories, carbonate chemistry and, critically, mechanisms by which food is supplied to the benthos. At present, nutrient and carbonate system data are primarily only available from global studies such as the World Ocean Atlas (WOA)<sup>15</sup> and the GLObal Ocean Data Analysis Project (GLODAP)<sup>16</sup>, and while useful for global assessments, provide very limited fine-scale spatial and temporal coverage that would describe a detailed baseline of the physicochemical environment that these CWC reef organisms experience. McGrath *et al.*<sup>17</sup> analyzed data from local and World Ocean Circulation Experiment (WOCE) cruises for the Rockall Trough between 1991–2010, providing a longer-term temporal analysis of the carbonate system at a more local scale, however the main focus was on the water column structure and change through time, as opposed to the CWC reef environmental conditions. The WOA and GLODAP datasets have been used to provide broad environmental envelopes for conditions that CWCs could exist on a global scale [e.g.<sup>4</sup>], but they are more limited in their use for regional analysis. Lunden *et al.*<sup>18</sup> provided a comprehensive survey of carbonate chemistry measurements specifically surrounding CWC reefs in the Gulf of Mexico, and Flögel *et al.*<sup>19</sup> more recently provided a summary of carbonate chemistry measurements for CWC in the wider North Atlantic region. However, in general fine-scale data is still hard to come by for these important organisms and their habitats, yet these CWC exist in highly dynamic environments, and their local distribution may be associated with this



natural variability. In the present study, we aim to assess the variability of nutrient and carbonate system dynamics across a range of temporal and spatial scales at four sites of known (but different) CWC reef habitats in the northeast Atlantic, representing a large diversity of CWC habitats surveyed in one research expedition.

The Rockall Bank is situated in the northeast Atlantic, approximately 400 km west of the Outer Hebrides (Fig. 1a). The depth ranges from over 1000 m at the base of the Bank, to 200 m across much of the top of the bank. Oceanic banks such as the Rockall Bank are characteristic in deviating major ocean currents to run along their flanks<sup>20</sup>, and these hydrodynamic regimes facilitate colonisation of CWC reefs<sup>21,22</sup>. The flanks of the Rockall Bank are known to contain extensive CWC reef habitats<sup>22,23</sup>. Two such sites are the Logachev coral carbonate mounds on the southwest flank<sup>24</sup>, and a site on the northwest flank (Fig. 1a, b), the Pisces site, first examined by Wilson<sup>21</sup> using the *Pisces III* submersible in 1973 (Fig. 1a), which includes a benthic ecosystem incorporating 'Wilson ring' patches of *Lophelia pertusa* reef habitat (Fig. 1c). Coral carbonate mounds, such as those at the Logachev site (Fig. 1d), are formed from successive periods of interglacial coral growth, whereas CWC patches (e.g. Pisces) and reefs (e.g. Mingulay Reef Complex) are 'single generation' Holocene accumulations<sup>25,26</sup>. Living reefs have been found at depths from 400 to 800 m at Logachev and from 200 to 400 m at Pisces. To contrast these deeper reefs, the third site is the Mingulay Reef Complex (MRC), a shallow CWC reef area consisting of a number of individual reefs (Fig. 1e), including Mingulay Area 01 (MA01) and Banana reef. The MRC is located on the European continental shelf, east of the Outer Hebrides, Scotland (Fig. 1a), where living reefs are found at depths from 120 to 190 m<sup>27,28</sup>. The final site was the Hebrides Terrace Seamount (HTS), which is found in approximately 2000 m water depth near the continental slope (Fig. 1a). Novel visual surveys of the seamount benthos have revealed previously unknown 'coral garden' habitats some of which are structured by the colonial scleractinian *Solenastrea variabilis* (Fig. 1f).

In the present study, additional focused sampling was carried out over a tidal cycle at three stations (MA01, 'Logachev South (LS)' and 'Logachev North (LN)', Fig. 1) to investigate the influence of the fine-scale ocean hydrodynamics on the environmental conditions at the depth of the CWC reefs. At the MRC, there is a known tidally-driven downwelling, and the detailed dynamics of the biogeochemical conditions of that site are described in Findlay *et al.*<sup>29</sup> therefore, only the relative variability is summarised here. In the region of the southwest Rockall Trough, containing the Logachev sites, there are known diurnal internal waves which cause vertical displacement of water masses resulting in relatively large fluctuations in temperature and salinity<sup>30</sup>. Carbonate and nutrient dynamics were therefore measured over a tidal period for both north (LN) and south (LS) of one of the coral carbonate mounds at Logachev.

## Results

**Temperature, salinity & water masses.** The northeast Atlantic is a complex region with numerous water masses. The MRC showed distinctly different temperature and salinity properties from all the other sites, which was primarily due to the coastal influence, and addition of freshwater run-off (Fig. 2). All the other sites (Logachev, Pisces and HTS) surrounding the Rockall Bank and Trough area, showed relatively similar properties throughout the water column (Fig. 2). The surface water (SW, Fig. 2) was indicated by an increase in temperature, but with little change in salinity. Below the surface water layer was found predominantly East North Atlantic Water (ENAW, Fig. 2), at depths between about 200 m to 700 m. Only Logachev and HTS were deeper than 700 m. At Logachev, below 700 m, Wyville-Thomson Overflow Water (WTOW, Fig. 2) was identified<sup>20</sup>, and at HTS, the WTOW was present at depths down to around 1200 m. Below 1200 m the water was influenced by colder fresher Labrador Sea Water (LSW,

Fig. 2). The water mass properties used here are taken from McGrath *et al.*<sup>20</sup> specifically for the Rockall Trough region.

**Fluorescence (chlorophyll), oxygen & particle attenuation coefficient ( $C_p$ ).** Chlorophyll fluorescence and  $C_p$  were correlated at all sites, such that as fluorescence increased,  $C_p$  increased (overall slope  $\beta = 0.67$ ,  $r = 0.509$ ,  $p < 0.0001$ , supplementary Fig. S1 online). The slope of the fluorescence- $C_p$  relationship was significantly different for each site (MRC  $\beta = 0.644$ , Logachev  $\beta = 0.3724$ , HTS  $\beta = 0.8143$  and Pisces  $\beta = 1.946$ ; supplementary Fig. S2 online). At MA01 there was a second increase in  $C_p$  towards the reef, which did not have a concomitant increase in chlorophyll (labeled as 'A' in Supplementary Fig. S1 online). This increase at depth was also evident at Logachev and at the HTS, and is likely to be due to resuspension of particulate matter from the seabed. There was also a deviation from the general trend in the surface waters at Pisces and the HTS, where fluorescence decreased without  $C_p$  decreasing (labeled as 'B' in Supplementary Fig. S1 online). At these sites there was clear evidence of a coccolithophore bloom in the upper water column at this time (late May-Early June); therefore this signal may represent particulates produced from both coccoliths and organic particles during the blooms at these sites.

Dissolved oxygen ranged from 206.1 to 288.8  $\mu\text{mol L}^{-1}$  across all sites and in all cases was seen to decrease with depth. Oxygen saturation ranged between 70 and 90% at the depths where the CWC reefs were located. The shallower sites did not reach as low oxygen concentrations as the deeper sites (dissolved oxygen was 250.3–286.9  $\mu\text{mol L}^{-1}$  at the MRC vs. 206.1–268.2  $\mu\text{mol L}^{-1}$  at Logachev), although there was still a removal of oxygen at the depths of the reefs. At the HTS, an oxygen minimum (203.6  $\mu\text{mol L}^{-1}$ ) was observed at about 1025 m, which corresponded approximately to the depth at the top of the seamount. Below this oxygen minimum, DO increased again to 257.5  $\mu\text{mol L}^{-1}$  at about 1900 m.

**Nutrients and the carbonate system.** Nitrate, silicate and phosphate concentrations increased with depth at all sites (Fig. 3). Surface nitrate and phosphate concentrations were lowest at MA01 (2.2  $\mu\text{M}$  and 0.3  $\mu\text{M}$ , respectively) whereas at Logachev and Pisces, the concentrations were still relatively high in the surface layers ( $>4 \mu\text{M}$  and  $>0.4 \mu\text{M}$ , respectively) (Table 1).

Dissolved inorganic carbon ( $C_T$ ) increased with depth at all sites, even when normalized to salinity ( $nC_T$ ) (Fig. 4).  $A_T$  was generally more stable through the water column, although there was greater variation through time. When normalized to salinity ( $nA_T$ ), each site showed a slightly different pattern in alkalinity with depth (Fig. 4). At MA01 and Banana reef there was, on average, a small decrease in  $nA_T$  with depth ( $\Delta nA_T$  (from surface to the depth of the reef) =  $\sim 8 \mu\text{mol kg}^{-1}$  and  $\sim 5 \mu\text{mol kg}^{-1}$ , respectively). At Logachev, the water column was generally well mixed with respect to  $nA_T$  above 450 m, below which it began to increase from about 2285  $\mu\text{mol kg}^{-1}$  to a maximum of 2320  $\mu\text{mol kg}^{-1}$  at 700 m. The HTS showed a slight decrease from the surface to 250 m ( $\sim 2310 \mu\text{mol kg}^{-1}$  to  $\sim 2290 \mu\text{mol kg}^{-1}$ ), and remained stable until below 1000 m when it began to increase again to  $\sim 2310 \mu\text{mol kg}^{-1}$  at 1500 m. At Pisces there was an increase in  $nA_T$  with depth, however, this appears to be driven by a decrease in alkalinity in the surface waters as the result of calcification from a coccolithophore bloom that was occurring at the time of sampling.

Formation and remineralisation of organic matter is generally assumed to occur at a C:N:P ratio (the Redfield ratio) of 106:16:1<sup>31</sup>. Across all sites the  $nC_T$ :P ratio was lower than the Redfield ratio, at approximately 75:1 (Fig. 5), while the N:P ratio was much closer to the Redfield ratio at 15.7:1 (Fig. 5). Therefore again indicating an overall signal of carbon addition, although this signal is influenced by the greater sampling effort that occurred at Logachev (Fig. 5).  $C_T$  also increased with decreasing temperature by approximately 15  $\mu\text{mol kg}^{-1} \text{ } ^\circ\text{C}^{-1}$  across all sites except for



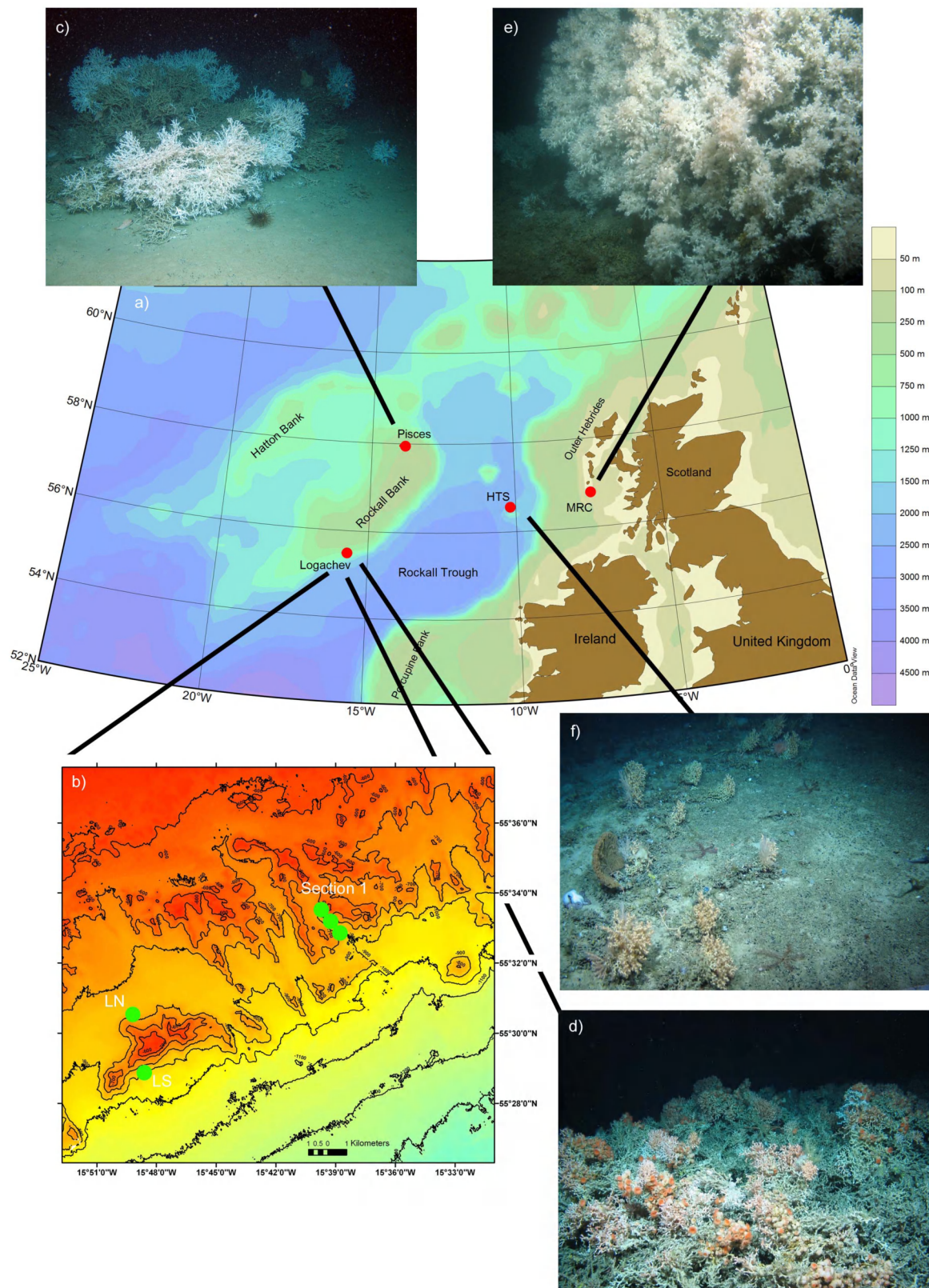


**Figure 1** | Map and example habitats of the sites studied in the northeast Atlantic during the ‘Changing Oceans’ expedition: (a) map (produced using ODV) showing the location of the four main sites: MRC = Mingulay Reef Complex, HTS = Hebrides Terrace Seamount, Logachev, and Pisces; (b) bathymetric map of the Logachev area (produced using ArcGIS 9, ESRI), highlighting the location of the fine-scale study areas LS = Logachev South, LN = Logachev North, and Section 1; (c) example of the ‘Wilson ring’ coral patches at Pisces; (d) example of the large coral carbonate mounds topped with large *Lophelia pertusa* structures at Logachev; (e) example of the shallower *L. pertusa* reefs at the MRC; and (f) example of the ‘coral garden’ habitats some of which are structured by the colonial scleractinian *Solenosmilia variabilis* at the HTS. Photographic images taken during Changing Oceans Expedition 2012 (RRS James Cook cruise 073). Images c, d, e courtesy Heriot-Watt University. Image f courtesy Heriot-Watt University and the Joint Nature Conservation Committee.

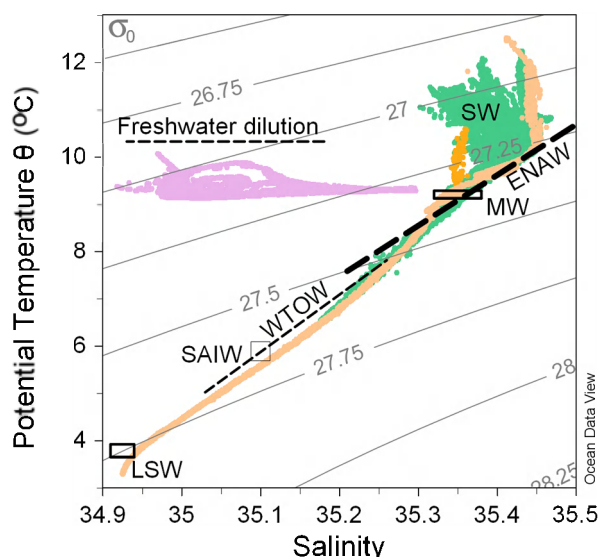


**Figure 2** | T-S plot with isopycnals, for the four main reef locations also showing the relevant water masses either as mixing lines (East North Atlantic Water (ENAW) and Wyville-Thomson Overflow Water (WTOW)) or boxes (Mediterranean Water (MW), Sub-Arctic Intermediate Water (SAIW) and Labrador Sea Water (LSW)), taken from McGrath *et al.* (2012b). Surface water (SW) and coastal freshening (freshwater dilution) are also indicated. Isopycnals are drawn in light grey. In colour, data points are marked as: Mingulay Reef Complex (MRC) = purple, Logachev mounds = green, Pisces = dark orange, and Hebrides Terrace Seamount (HTS) = pale orange.

Mingulay, which showed a shift in  $C_T$  without a significant change in temperature (Fig. 5).

Statistically,  $C_T$  and  $A_T$  profiles were significantly affected by the sites themselves (ANOSIM,  $Global R = 0.326$ ,  $p = 0.01$ ). However, pairwise tests revealed MA01 and Banana reef were not statistically different ( $R = -0.02$ ,  $p = 0.57$ ), but MA01 was most distinct from all the other sites ( $p = 0.01$  in all cases). Furthermore, when depth included as a factor, MA01 is distinct from all sites ( $p < 0.012$  in all cases), except Banana reef ( $p = 0.598$ ). Between the other three sites (Logachev, Pisces and HTS), only Logachev and Pisces were statistically distinct ( $R = 0.255$ ,  $p = 0.045$ ).

$pH_T$  ranged from 8.19 to 7.92, decreasing with depth from an average  $pH$  of  $>8.10$  in the upper mixed layer.  $\Omega_{Aragonite}$  ranged from 1.1 to 2.6 across all sites and depths; again, generally showing a decrease in saturation state with depth at all sites (Fig. 4).

$n_{C_T}$  and  $\Omega_{Aragonite}$  both had strong significant correlations with oxygen % saturation. The relationships are provided here for Logachev site only; these relationships are explored in more detail in supplementary information (S2) online:

$$n_{C_T} = -2.3168 * OxySat + 2318.2, \quad (1)$$

( $r = 0.9079$ ,  $df = 169$ ,  $p < 0.001$ ; Fig. 6d)

$$\Omega_{Aragonite} = 0.0229 * OxySat - 0.1257, \quad (2)$$

( $r = 0.8381$ ,  $df = 169$ ,  $p < 0.01$ )

**Logachev fine-scale dynamics.** Data from a transect ('Section 1' Fig. 1a) onto the Rockall Bank in the Logachev region shows the fine-scale spatial variability, and indications of potential upwelling of deeper waters by internal waves onto the carbonate mounds, where CWC are located between 800 and 600 m (Fig. 6). At both LS and LN, internal waves influence temperature and salinity most

significantly below 500 m<sup>30</sup>, as evidenced in our dataset: At LS, the daily  $\Delta$ temperature and  $\Delta$ salinity at 500 m was 0.71°C and 0.06 psu; at 600 m was 0.90°C and 0.07 psu; and at 800 m was 2.05°C and 0.14 psu. At LN, the daily  $\Delta$ temperature and  $\Delta$ salinity at 500 m was 0.78°C and 0.06 psu; at 600 m was 0.88°C and 0.06 psu; and at 800 m was 1.77°C and 0.11 psu. Nitrate, phosphate, silicate and  $n_{C_T}$  all showed corresponding changes through time in the water column below 500 m, while  $n_{A_T}$  showed very little variability through a daily cycle, although fewer discrete samples for  $C_T$ ,  $A_T$  and nutrients were taken compared to the CTD data. For example, at both LS and LN, at the depth of 600 m,  $n_{C_T}$  varied by  $\sim 40 \mu\text{mol kg}^{-1}$  through the 12 h period, while  $n_{A_T}$  varied by only  $14 \mu\text{mol kg}^{-1}$ . The change in  $C_T$  caused a change in the other carbonate system parameters, for example aragonite saturation state varied by  $\sim 0.2$  over the period. Because of the strong relationships with oxygen saturation (%), and the more frequent data available from the oxygen sensor mounted on the CTD, this relationship (Eq. 1) was used to calculate full profiles for  $n_{C_T}$  over the 12 h periods at the two Logachev sites (Fig. 6).

## Discussion

Empirical observations for nutrient and carbonate system dynamics are shown for a number of CWC habitats: one coral carbonate mound, two cold-water coral (CWC) reefs, and one Seamount found in the northeast Atlantic region (Fig. 1). The dissolved inorganic carbon ( $C_T$ ) and alkalinity ( $A_T$ ) concentrations are within 1.5% and 1% respectively of data extracted from the GLODAP database (comparing GLODAP gridded data at 55.5 N, 15.5 W<sup>16</sup> with mean values from Logachev at 55.5 N, 15.7 W).

The environmental conditions at the study sites predominantly fall within the global envelope for CWCs described in Davies *et al.*<sup>5</sup>. The nutrient concentrations fall within the range prescribed for the NE Atlantic<sup>5</sup>; however, here we provide data for the carbonate system parameters that were not previously available at a high resolution of sampling. Flögel *et al.*<sup>19</sup> recently published a comparison of available carbonate system data for CWC in the North Atlantic, including the Mediterranean, which fits well with our data collected at similar locations, and supports earlier data from this region [e.g.<sup>11,32</sup>]. Flögel *et al.*<sup>19</sup> suggest coral "quality" is associated with a seawater density range similar to that originally described by Dullo *et al.*<sup>4</sup> and highlighted in niche width models by Davies *et al.*<sup>5</sup>, but also that low quality CWCs are exposed to  $C_T$  concentrations  $< 2170 \mu\text{mol kg}^{-1}$ .

A number of recent publications provide a wider comparison of carbonate and nutrient conditions across sites of known CWC reefs, between the NE Atlantic [our data<sup>5,19</sup>], the Mediterranean, the Gulf of Cadiz, and Mauritania<sup>11,19,32</sup>, the Gulf of Mexico (GoM)<sup>18</sup>, Chilean fjords<sup>32,33</sup>, the Marmara Sea and the Tasman Seamount<sup>32</sup> (Table 2). CWC reefs in the NE Atlantic (excluding the Mediterranean) appear to experience slightly lower  $C_T$  concentrations than CWC reefs in the GoM, but similar levels of  $A_T$ , which results in the GoM experiencing, on average, lower  $\Omega_{Aragonite}$  than in the NE Atlantic (Table 2). Although no assessment of CWC quality is provided by Lunden *et al.*<sup>18</sup>,  $C_T$  is higher than the proposed limit of  $2170 \mu\text{mol kg}^{-1}$ . Furthermore, Lunden *et al.*<sup>18</sup> found no significant relationship between skeletal density and  $\Omega_{Aragonite}$ , which suggests these conditions were not limiting for calcification. The Chilean fjords have similar and slightly lower levels of  $C_T$  but significantly lower salinity and consequently significantly lower  $A_T$ , and again therefore experience lower  $\Omega_{Aragonite}$  than the NE Atlantic (Table 2). However, different coral species (*Desmophyllum dianthus*) are abundant at the Chilean sites and this also needs to be taken into account when assessing CWC sensitivities.

While these datasets provide just one or two data points for each location (for an average or "spot" condition), we highlight here that measuring through time at one site provides as much variability as is found across the sites (Table 1 and Table 2). For example, at MA01,



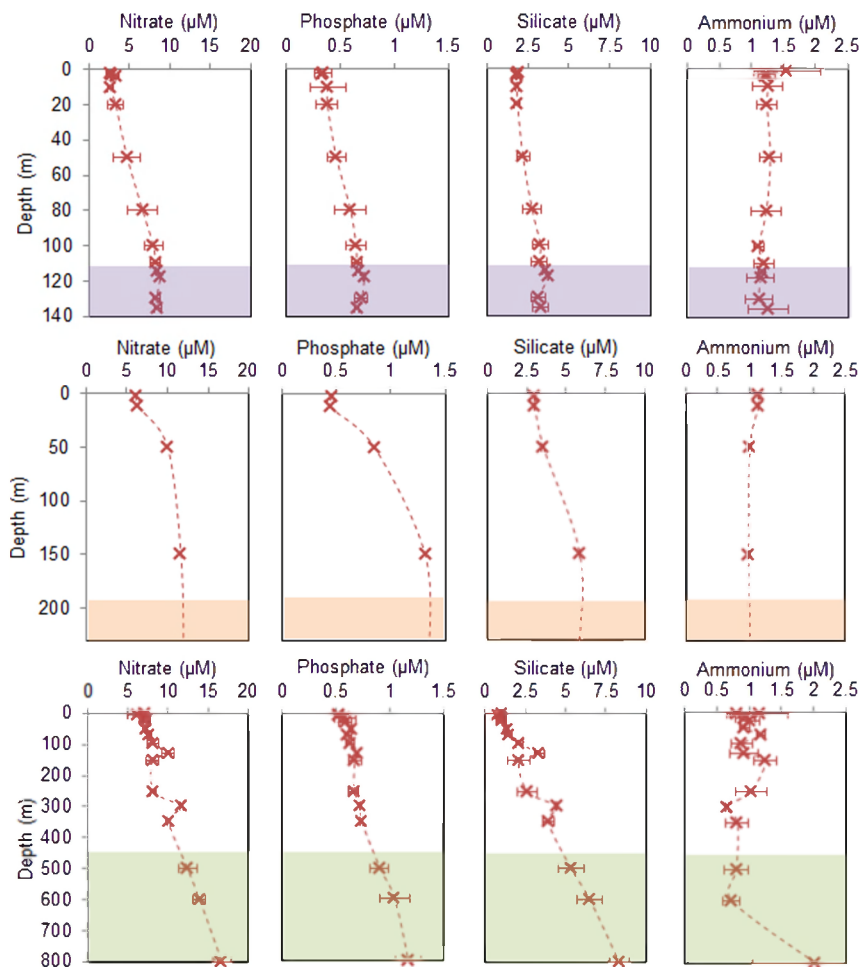


**Figure 3** | Average (mean  $\pm$  standard deviation) profiles through the water column at three of the sites: (first row) Mingulay Reef Complex, (second row) Pisces, and (third row) Logachev, for (first column) nitrate ( $\mu\text{M}$ ), (second column) phosphate ( $\mu\text{M}$ ), (third column) silicate ( $\mu\text{M}$ ), and (fourth column) ammonium ( $\mu\text{M}$ ). Also showing the depth ranges where CWC reefs were observed during ROV dives (colored areas on each graph). No nutrient data were collected at the Hebrides Terrace Seamount. Note the depth scale changes.

the localised downwelling caused  $C_T$  to decrease below the lowest reported value from Flögel *et al.*<sup>19</sup>, to  $<2090 \mu\text{mol kg}^{-1}$ , with a total  $C_T$  range at MA01 of  $40 \mu\text{mol kg}^{-1}$ . At the Logachev site, upwelling and internal waves caused  $C_T$  to increase above the highest reported

value from Flögel *et al.*<sup>19</sup>, to  $>2185 \mu\text{mol kg}^{-1}$ . Across the Logachev site we found a total  $C_T$  range of  $58 \mu\text{mol kg}^{-1}$ , which is nearly double the reported range for the Western Rockall Bank ( $24 \mu\text{mol kg}^{-1}$ ), for CWC given a quality category of CI-CII<sup>19</sup>. Interestingly, the

**Table 1** | Range (minimum – maximum) of environmental conditions observed at the each site through the whole water column: Mingulay Area 01 (MA01), Banana Reef, Logachev, Pisces, and Hebrides Terrace Seamount (HTS).  $\text{pH}_T$  and  $\Omega_{\text{aragonite}}$  were calculated from  $C_T$  and  $A_T$ , salinity, temperature, phosphate and silicate (when available), using CO2sys.  $C_T$  and  $A_T$  have been normalised ( $nC_T$  and  $nA_T$ ) to salinity of 35, to compare across sites. nd = no data available

	Site				
	MA01	Banana	Logachev	Pisces	HTS
Dates	21–23/05/12	24/05/12	26/05–06/06/12	07/06/12	09/06/12
Max. depth (m)	135	130	910	220	1930
$nC_T$ ( $\mu\text{mol kg}^{-1}$ )	2062–2124	2067–2110	2075–2172	2052–2131	2068–2168
$nA_T$ ( $\mu\text{mol kg}^{-1}$ )	2266–2321	2298–2317	2263–2321	2258–2308	2289–2319
$\text{pH}_T$	8.03–8.19	8.06–8.14	7.94–8.10	8.01–8.11	7.92–8.13
$\Omega_{\text{aragonite}}$	1.92–2.62	2.05–2.42	1.35–2.35	1.82–2.34	1.11–2.58
$\text{HCO}_3^-$ ( $\mu\text{mol kg}^{-1}$ )	1878–1994	1908–1969	1925–2058	1905–2004	1910–2043
$\text{CO}_3^{2-}$ ( $\mu\text{mol kg}^{-1}$ )	130–173	135–160	103–157	123–155	105–170
$\text{NO}_3^-$ ( $\mu\text{mol L}^{-1}$ )	2.18–9.00	nd	4.10–18.82	6.14–11.65	nd
$\text{NO}_2^-$ ( $\mu\text{mol L}^{-1}$ )	0.04–0.43	nd	0.02–0.31	0.04–0.44	nd
$\text{PO}_4$ ( $\mu\text{mol L}^{-1}$ )	0.26–3.59	nd	0.48–3.04	0.44–1.31	nd
$\text{SiO}_4$ ( $\mu\text{mol L}^{-1}$ )	1.67–3.74	nd	0.68–9.40	3.01–5.87	nd
$\text{DO}$ ( $\mu\text{mol L}^{-1}$ )	250.3–286.9	255.3–288.8	206.1–268.2	251.2–274.9	207.2–270.8
Fluorescence ( $\mu\text{g Chl L}^{-1}$ )	0.04–0.50	0.05–0.30	0.02–0.37	0.04–0.87	0.02–1.17

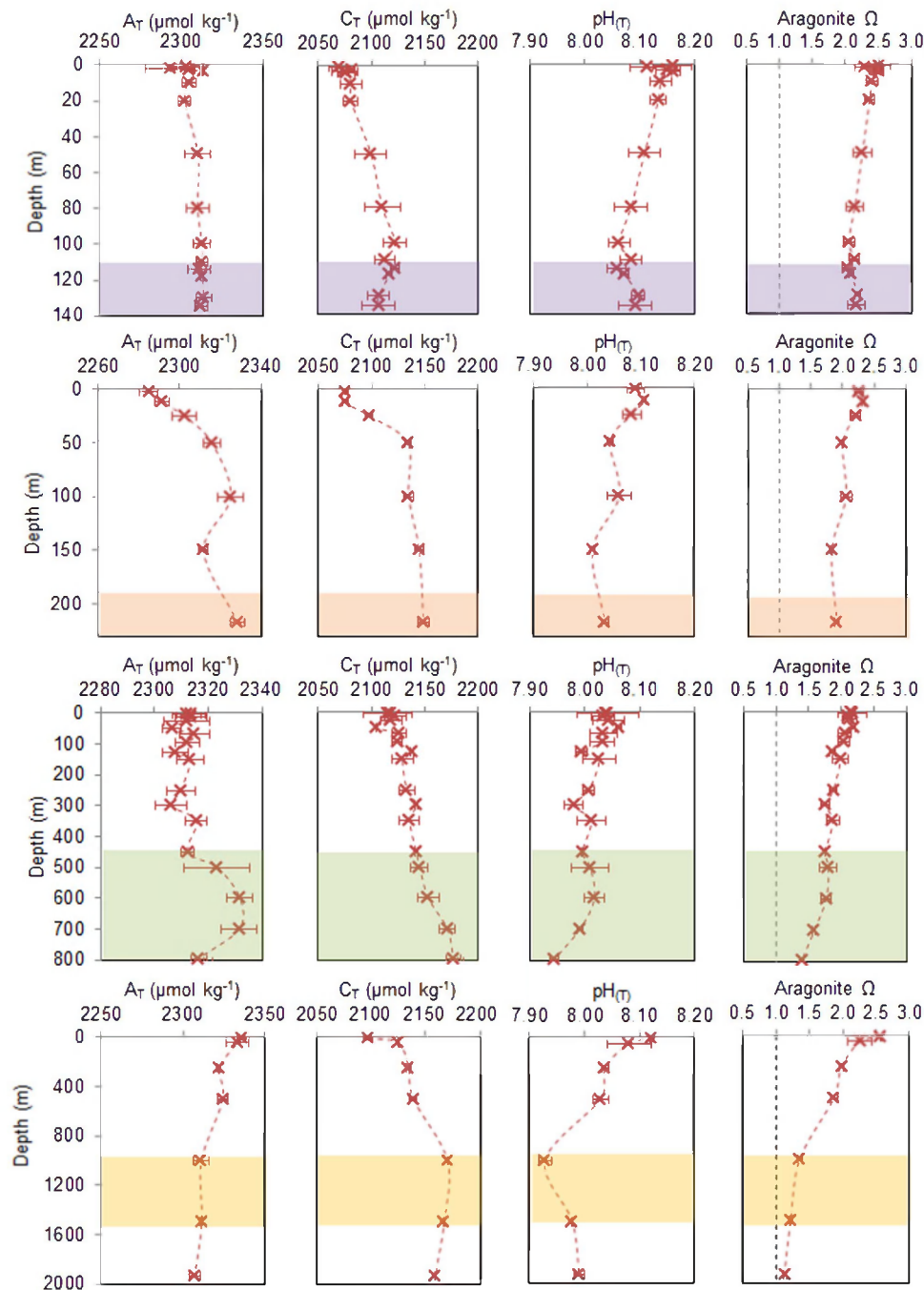


**Figure 4** | Average (mean  $\pm$  standard deviation) profiles through the water column at all sites: (first row) Mingulay Reef Complex, (second row) Pisces, (third row) Logachev, and (fourth row) Hebrides Terrace Seamount, for (first column) total alkalinity ( $A_T$ ), (second column) dissolved inorganic carbon ( $C_T$ ), (third column) pH (total scale), and (fourth column) aragonite saturation state ( $\Omega_{\text{aragonite}}$ ). Also showing the depth ranges where CWC reefs were observed during ROV dives (colored areas on each graph). Note the depth scale changes.

majority of CWC reefs attributed to quality category CIII<sup>19</sup> were found predominantly in the Mediterranean, which naturally has high temperatures and salinities, but additionally in Mauretania and in the Gulf of Cadiz, both of which also have higher temperatures than the majority of CI and CII sites<sup>19</sup>.

$\text{pH}_T$  and  $\Omega_{\text{Aragonite}}$  varied by approximately 0.27 and 1.51 respectively (Table 1), over the spatial (and depth) region investigated here, although the hydrodynamics clearly increased the variability for  $\text{pH}_T$  and  $\Omega_{\text{Aragonite}}$  at the sites where finer time-scale measurements were carried out (MA01, LS and LN; Table 1). Indeed, using *in situ* lander measurements, Mienis *et al.*<sup>30</sup> described the fine-scale dynamics at the southwest Rockall Trough margin (Logachev region) over a

longer sampling period (about 1 year) and found that the water current speeds peaked just before or at the same time as the peaks in temperature and salinity. The physical conditions (temperature and salinity) in our dataset correspond to the observations of Mienis *et al.*<sup>30</sup>, where internal waves cause a diurnal shift in the physical conditions. The transport of  $C_T$  and nutrients, along with sediments and particles *via* these internal waves could prevent a build-up of high  $\text{CO}_2$ , low oxygen conditions around the CWC reefs, flushing them with fresh material, nutrients and lower  $\text{CO}_2$  conditions over a diurnal cycle. Therefore on a fine-scale these hydrodynamics create additional variability not accounted for by cruises that only sample once per station. Indeed Flögel *et al.*<sup>19</sup> suggest a narrower range of

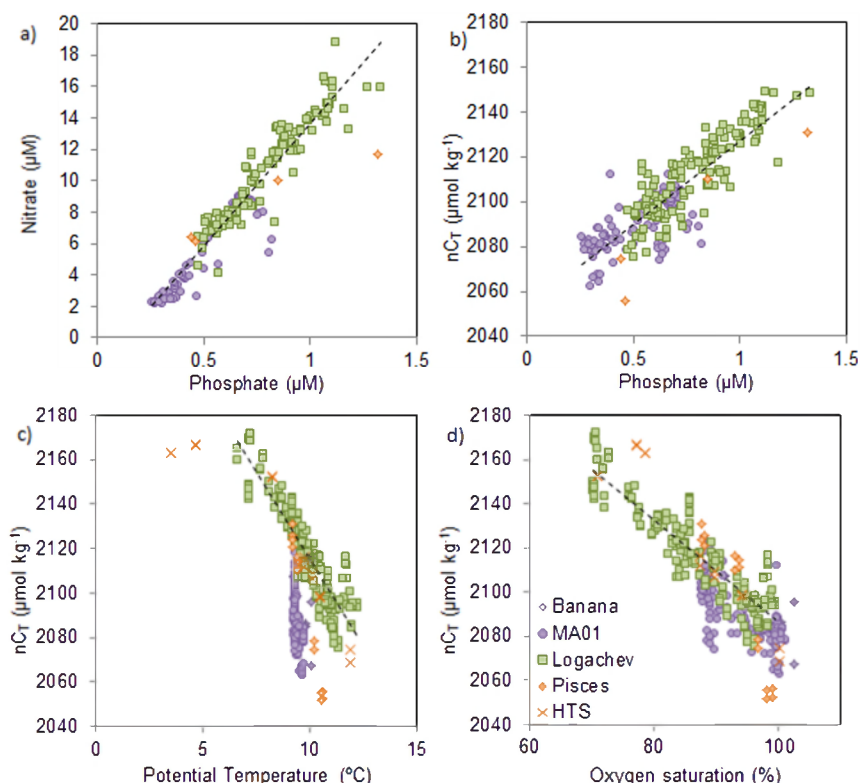


**Figure 5 | Relationships between (a) nitrate and phosphate, (b)  $nC_T$  and phosphate, (c)  $nC_T$  and potential temperature, and (d)  $nC_T$  and oxygen saturation (%).** Coloured symbols represent the different sites (as in Figure 2); dashed black lines in each plot represents the line of best fit to the data.

conditions could be considered if Mingulay Reef is excluded from their assessment because of its downwelling impacts, yet the very nature of this downwelling contributes to a higher variability in chemical components such as  $C_T$  and nutrients, and consequently impacts the local environment for CWCs and associated biodiversity<sup>29</sup>.

Kenyon *et al.*<sup>24</sup>, suggested that CWC reefs in the North Atlantic were found in the Oxygen Minimum Zone (OMZ). An OMZ usually corresponds with high  $C_T$  and  $pCO_2$  because OMZs arise from remineralisation of organic matter and therefore consumption of oxygen, and release of  $CO_2$ . Our dataset shows a strong negative relationship between oxygen % saturation and  $nC_T$ , such that at the lowest oxygen levels there was highest  $nC_T$  concentration (e.g.  $nC_T \approx 2160 \mu\text{mol kg}^{-1}$  at 70% oxygen saturation). Correspondingly, these low DO areas also exhibit the lowest pH and low  $\Omega_{\text{Aragonite}}$  (e.g. at 70% oxygen saturation,  $pH \approx 7.94$  and  $\Omega_{\text{Aragonite}} \approx 1.3$ , although  $\Omega_{\text{Aragonite}}$  continued to decrease with depth after the OMZ because of the influence of low saturation state in the LSW). CWC reefs therefore appear to be thriving in conditions that are conventionally considered unsuitable for many organisms, particularly calcifiers, and this confirms that the variable physicochemical environment found here is not limiting CWC reef growth. The natural fluctuations in the physicochemical conditions (including oxygen, carbon, nutrients and food supply), driven by large hydrodynamics, may provide flexibility for these organisms, giving them increased adaptation potential for surviving a range of conditions, as has been found with warm-water corals and temperature<sup>34</sup>. This naturally fluctuating environment could help to explain the high levels of variability found in CWCs ocean acidification experiments, especially as several recent laboratory experiments CWCs are able to continue calcifying under high  $CO_2$ , low  $\Omega_{\text{Aragonite}}$  conditions [e.g.<sup>35–37</sup>].

Interestingly, the carbonate mounds (between 400 and 700 m water depth) at Logachev appear to provide an additional, albeit relatively small, carbon (alkalinity) source to the water column, com-

pared to the other sites that consist of coral habitats but do not have carbonate mounds present. On average,  $nC_T$  steadily increased over this depth range at Logachev yet normalized alkalinity remained the same, hence the seawater pH was somewhat buffered and therefore also remained relatively uniform across the depth range of the mound. The caveat to this interpretation is the different end-members of  $C_T$  and  $A_T$  associated with different water masses; given the complex physical oceanography and diversity of water masses and potential mixing in this area, further work is required to elucidate if this apparent alkalinity increase is really from the carbonate mounds or if it is from high alkalinity water masses, for example flowing south from the Arctic, which has a different set of implications in the context for global climate change and ocean acidification.

Carbonate system measurements from the deepest samples taken at Logachev and at the Hebrides Terrace Seamount, show that the aragonite saturation state approaches 1.2–1.3 across the Rockall Trough at approximately 1000 m, decreasing to near 1.0 at 1500 m. The present day depth of the aragonite saturation horizon (ASH) in the NE Atlantic is therefore similar, or in localised areas shallower, than in model projections for the North Atlantic (e.g. the 1994 depth was approximately 2500 m<sup>38</sup>). Future model projections for the ASH show it shoaling to 600–800 m by mid-century (2046–2065) and then further surface-ward to around 200 m by the end of century (2080–2099)<sup>38</sup>. Indeed, McGrath *et al.*<sup>17</sup>, show that  $C_T$  has increased, resulting in an equivalent decrease in pH of  $0.040 \pm 0.003$  units in the sub-surface waters, over the 19 years that were investigated for the Rockall Trough region. This was concomitant with a decrease in saturation state of both aragonite and calcite and a shoaling of the ASH.

While it appears CWC reefs are naturally exposed, and thereby appear tolerant to, a wide range of conditions, the deeper reefs could be at risk of dissolution or be affected by a shift in their physiology as a result of hypercapnia<sup>39,40</sup>. Even if the corals themselves have a degree of acclimation in response to high  $CO_2$  conditions<sup>32,35–37,39,40</sup>,

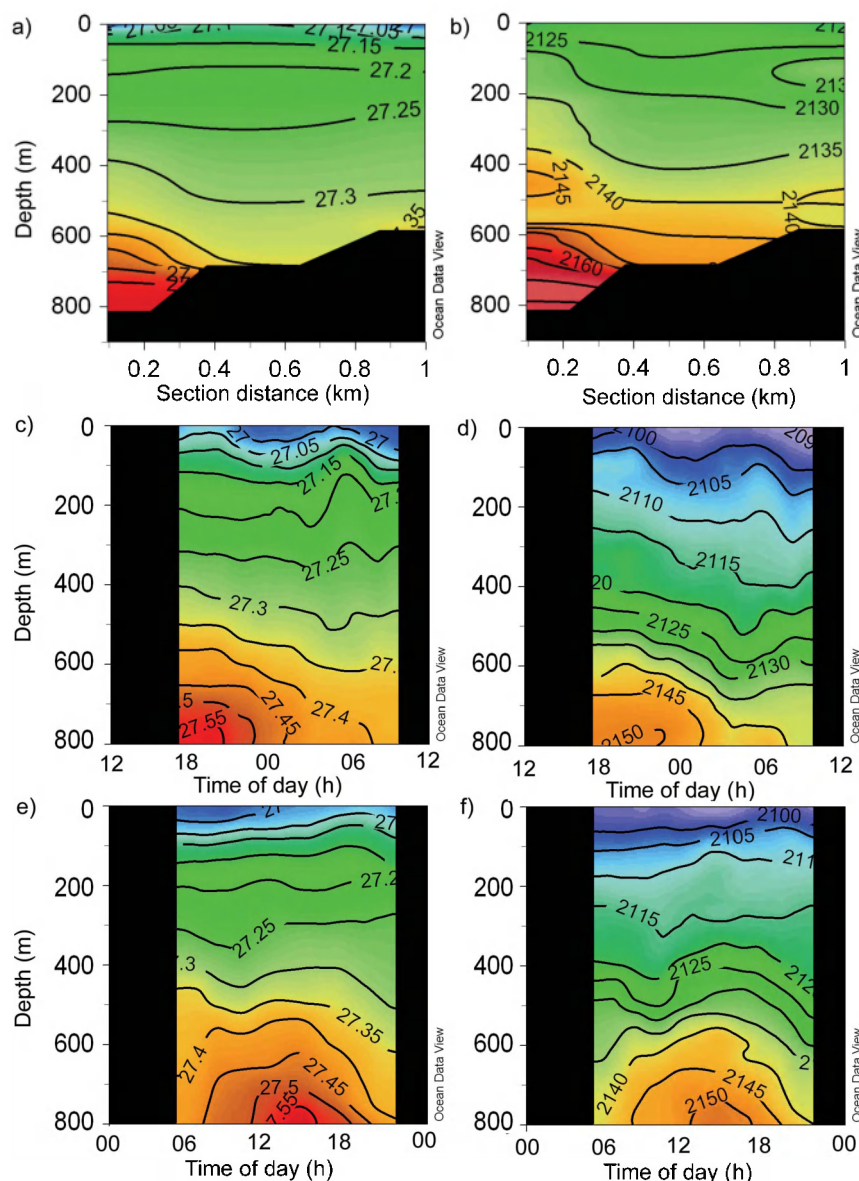


**Figure 6** | Profiles of density (a, c, e) and  $nC_T$  ( $\mu\text{mol kg}^{-1}$ ) estimated from Oxygen % saturation (see text, equation 1) (b, d, f) across a transect ‘Section 1’ up onto the Rockall Bank (a and c), and through time, over one 24 hour period, for stations at Logachev North ‘LN’ (c and d) and Logachev South ‘LS’ (e and f). See figure 1 for location of the transect and the two stations LS and LN.

**Table 2** | The range (published min-max) of environmental conditions at different regions, specifically at the depth and site of known CWC reefs, comparing data from this study with data available in the literature<sup>5,11,19,32,33</sup>

Location	NE Atlantic (this study)	NE Atlantic	Gulf of Cadiz	Mauretania	Mediterranean	Gulf of Mexico	Chilean Fjords	Marmara Sea	Tasman Seamount
Depth (m)	120–1000	100–950	606–1322	451–568	89–850	307–620	20–200	932	1050
Temperature ( $^{\circ}\text{C}$ )	7.2–10.0	5.9–10.6	9.2–11.0	9.7–11.7	12.8–16.8	nd	10.6–12.5	14.5	4.59
Salinity	35.1–35.4	35.0–35.7	35.6–36.0	35.2–35.4	37.8–38.8	35.05*	31.7–33.0	38.8	34.4
$A_T$ ( $\mu\text{mol kg}^{-1}$ )	2299–2346	2287–2377	2332–2342	2314–2375	2520–2742	2259–2391	2136–2235	2610	2315
$C_T$ ( $\mu\text{mol kg}^{-1}$ )	2088–2186	2118–2174	2180–2200	2183–2240	2226–2349	2135–2231	2025–2188	2470	2218
$\Omega_{\text{Aragonite}}$	1.35–2.44	1.39–3.03	1.43–1.83	1.31–1.58	2.59–4.06	1.19–1.69	0.78–1.60	1.46	1.02
C-refs.		19	19	19	11,19,32	11	32,33	32	32
$\text{PO}_4$ ( $\mu\text{mol L}^{-1}$ )	0.6–1.5	0.4–1.6			0.20–0.41				
$\text{NO}_3$ ( $\mu\text{mol L}^{-1}$ )	4.1–18.8	8.0–23.4			nd				
$\text{NH}_4$ ( $\mu\text{mol L}^{-1}$ )	0.5–1.6	nd			0–0.29				
$\text{SiO}$ ( $\mu\text{mol L}^{-1}$ )	2.1–9.4	2.2–46.6			nd				
N-Refs.		5			11				

C-Refs. = References for carbon system data; N-Refs. = References for nutrient data; nd = no data reported.

\*Only mean salinity reported in<sup>11</sup>.





dissolution of the coral carbonate mounds, such as those found at Logachev, and any dead coral structure, which provides the hard substrate on which corals and abundant epifauna can grow<sup>41</sup>, could become unstable as the ASH shoals. Coupled with predicted increased efficiency of bio-eroding sponges<sup>42</sup> and a multitude of additional threats<sup>43</sup>, these deeper reefs could face significant threat of degradation. Furthermore, the differing rates of acidification occurring in the different water masses that are associated with these reefs (e.g. increased acidification rate in LSW compared with surface waters<sup>17</sup>) will also alter the regional threat to these important communities.

## Methods

A total of 30 CTD and rosette sampling casts were carried out across the sites (MRC, Logachev, Pisces and HTS (Fig. 1)) between 21<sup>st</sup> May and 9<sup>th</sup> June 2012<sup>44,45</sup> during the 'Changing Oceans Expedition 2012', on board the RRS *James Cook*, cruise JC073<sup>46</sup>. A Sea-Bird 911 plus CTD system (9plus underwater unit and Sea-Bird 11plus deck unit) was deployed with a Rosette water sampling unit, fitted with 10 L Niskin water bottles. Water samples were taken at discrete depths throughout the water column with the deepest samples being taken approximately 2 m above the reef (using altimeter information on-board the CTD). These samples are referred to as "immediately above the reef". Pre-cruise laboratory calibrations were performed on the conductivity, temperature and pressure sensors, all giving coefficients for linear fit. Also attached to the Rosette was a Sea-Bird 43 dissolved oxygen sensor, a Chelsea Aquatracka MKIII fluorometer (set to detect Chlorophyll  $\alpha$ : excitation wavelength of 430 nm and emission wavelength of 685 nm), and a Chelsea Aquatracka MKIII Transmissometer, which were used to measure dissolved oxygen, chlorophyll fluorescence, and particle attenuation coefficient ( $C_p$ ; measured at wavelength of 660 nm; e.g. Behrenfeld and Boss<sup>47</sup>, and references therein), respectively. Dissolved oxygen was calibrated against Winkler titrations<sup>48</sup> made on discrete water samples collected from a range of depths, and produced an offset between the titrations and sensor measurements of <1%. Because of the fine-scale of the hydrodynamics being assessed here, the up-cast raw data were used for the analysis and interpretation of the discrete measurements to match water column state at the time of bottle firing (see supplementary information S3 online for up-cast vs down-cast variability assessment). Further data processing was performed using the software SBE Data Processing (V7.21g) and for data visualization Ocean Data View (V4.3.7)<sup>49</sup> was used.

Seawater was collected from the Niskin bottles for the dissolved inorganic carbon ( $C_T$ ) and total alkalinity ( $A_T$ ) analysis. Samples were collected in borosilicate glass bottles with ground glass stoppers (50 mL), which were rinsed and filled according to standard procedures detailed in<sup>50</sup>. Samples were poisoned with 10  $\mu$ L mercuric chloride ( $HgCl_2$ ) and duplicate samples were taken from the same Niskin bottle. Samples were returned to the chemical laboratory onboard the RRS *James Cook*, where they were normalized to room temperature (approx. 24°C) and analyzed for  $C_T$  and  $A_T$  within 24 hours of collection.

$C_T$  was measured using a Dissolved Inorganic Carbon Analyzer (Apollo SciTech, Model AS-C3) calibrated using CO<sub>2</sub> Certified Reference Materials (Dickson, Batch 113). Duplicate measurements provided an estimate of measurement error, which was 0.2% across the entire dataset. An assessment of errors for each site is provided in supplementary information S4 online.  $C_T$  was corrected for the addition of  $HgCl_2$ .

$A_T$  was measured using the open-cell potentiometric titration method using an automated titrator (Apollo SciTech Alkalinity Titrator Model AS-ALK2). Calibration was made using CO<sub>2</sub> Certified Reference Materials (Dickson, Batch 113). Duplicate measurements were made for each sample, and the estimate of measurement error was 0.4% across the entire dataset. An assessment of errors for each site is provided in supplementary information S4 online.  $A_T$  was corrected for the addition of  $HgCl_2$ .

Seawater was collected for nutrient analysis from the CTD Niskin bottles directly after samples were taken for the carbon analysis. 50 mL of collected seawater was filtered (0.45  $\mu$ m acid-washed Millipore Fluoropore) into acid-cleaned, aged, 60 mL Nalgene bottles, duplicate samples were collected from each Niskin. Bottles were stored and shipped back frozen (−20°C) to Plymouth Marine Laboratory, where analysis was carried out<sup>51</sup> using a Bran and Luebbe AAIII segmented flow autoanalyzer for the colorimetric determination of inorganic nutrients: combined nitrate and nitrite<sup>52</sup>, nitrite<sup>53</sup>, phosphate<sup>53</sup>, and silicate<sup>54</sup>. Nitrate concentrations were calculated by subtracting nitrite concentration from the combined nitrate + nitrite concentration.

The remaining carbonate system parameters ( $pH_T$ ,  $pCO_2$ ,  $\Omega_{aragonite}$ ) were calculated from measured  $A_T$  and  $C_T$ , together with depth, temperature, salinity, silicate, and phosphate (when available), using the programme CO2SYS<sup>55</sup>, with dissociation constants from<sup>56</sup> refit by<sup>57</sup> and for KSO<sub>4</sub> from<sup>58</sup>.

In addition to temperature and salinity, three other major processes influence carbonate chemistry: organic matter formation and remineralisation, calcium carbonate calcification and dissolution, and air-sea gas exchange. At the depth of the CWC reefs described here, air-sea gas exchange is assumed to be negligible; therefore we assume that air-sea gas exchange only contributes to carbon dynamics in the surface waters. To remove the effects of salinity,  $C_T$  and  $A_T$  were normalized to a reference salinity ( $S^{ref} = 35$ ) using standard methods (see<sup>59</sup> for discussion of normalization options) and are denoted as  $nC_T$  and  $nA_T$ , respectively. For example, for measured  $A_T$  ( $A_T^{meas}$ ) and measured salinity ( $S^{meas}$ ):

$$nA_T = \frac{A_T^{meas}}{S^{meas}} \cdot S^{ref} \quad (3)$$

At the two Logachev stations LS and LN, CTD profiling was conducted continuously for a period of just over 12 hours at each site (first at LS and then at LN); with additional discrete samples taken at 500 m and 600 m: four times at (LS) and six times at (LN). At this site the deepest samples were taken immediately above the coral carbonate mounds (see supplementary Fig. S7 online). An ROV survey of the top of the carbonate mound revealed *Lophelia* reefs on the top of the mound.

An Analysis of Similarities (ANOSIM) test was conducted to assess similarities in the carbonate system and nutrients across the different sites, using Primer v6<sup>60</sup>. Correlations between variables was analyzed for statistical significance using Pearson's correlation coefficients, and in some cases the slopes were used to test for significant differences between regression lines.

- Dullo, W.-C. Coral growth and reef growth: a brief review. *Facies* **51**, 33–48 (2005).
- Hennige, S. J., Suggett, D. J., Hepburn, L., Pugsley, A. & Smith, D. J. Coral reefs of the Wakatobi: processes of reef growth and loss. *Marine Research and Conservation in the Coral Triangle: the Wakatobi Marine National Park*, Clifton, J., Unsworth, R. K. F. & Smith, D. J. (eds.), 27–44 (Nova, New York, 2010).
- Dorschel, B., Hebbeln, D., Rüggeberg, A. & Duloo, C. Carbonate budget of a cold-water coral carbonate mound: Propeller Mound, Porcupine Seabight. *Int. J. Earth Sci.* **96**, 73–83 (2007).
- Dullo, W.-C., Flögel, S. & Rüggeberg, A. Cold-water coral growth in relation to the hydrography of the Celtic and Nordic European continental margin. *Mar. Ecol. Prog. Ser.*, **371**, 165–176 (2008).
- Davies, A. J., Wisshak, M., Orr, J. C. & Roberts, J. M. Predicting suitable habitat for the cold-water coral *Lophelia pertusa* (Scleractinia). *Deep-Sea Res. I* **55**, 1048–1062 (2008).
- Silverman, J., Laza, B. & Erez, J. Effect of aragonite saturation, temperature, and nutrients on the community calcification rate of a coral reef. *J. Geophys. Res.* **112**, C05004, doi:10.1029/2006JC003770 (2007).
- Manzello, D. P. Ocean acidification hot spots: Spatiotemporal dynamics of the seawater CO<sub>2</sub> system of eastern Pacific coral reefs. *Limnol. Oceanogr.* **55**, 239–248 (2010).
- Santos, I. R., Glud, R. N., Maher, D., Erler, D. & Eyre, B. D. Diel coral reef acidification driven by porewater advection in permeable carbonate sands, Heron Island, Great Barrier Reef. *Geophys. Res. Lett.* **38**, L03604, doi:10.1029/2010GL046053 (2011).
- Gray, S. E. C., DeGrandpre, M. D., Langdon, C. & Corredor, J. E. Short-term and seasonal pH, pCO<sub>2</sub> and saturation state variability in a coral-reef ecosystem. *Global Biogeochem. Cycles* **26**, GB3012, doi:10.1029/2011GB004114 (2012).
- Anthony, K. R. N., Diaz-Pulido, G., Verlinden, N., Tilbrook, B. & Andersson, A. J. Benthic buffers and boosters of ocean acidification on coral reefs. *Biogeosci.* **10**, 4897–4909, doi:10.5194/bg-10-4897-2013 (2013).
- Maier, C., Watremez, P., Taviani, M., Weinbauer, M. G. & Gattuso, J.-P. Calcification rates and the effect of ocean acidification on Mediterranean cold-water corals. *Proc. Roy. Soc. B* **279**, 1716–1723, doi:10.1098/rspb.2011.1763 (2012).
- De Mol, et al. Cold-water coral habitats in the Penmarch and Guilvinec Canyons (Bay of Biscay): Deep-water versus shallow-water settings. *Mar. Geol.* **282**, 40–52 (2011).
- Rüggeberg, A., Flögel, S., Dullo, W.-C., Hissmann, K. & Freiwald, A. Water mass characteristics and sill dynamics in a subpolar cold-water coral reef setting at Stjærnsund, northern Norway. *Mar. Geol.* **282**, 5–12 (2011).
- Davies, A. J. et al. Short-term environmental variability in cold-water coral habitat at Viosca Knoll, Gulf of Mexico. *Deep-Sea Res. I*, **57**, 199–212 (2010).
- Murphy, P. P. et al. NOAA Atlas NESDIS 47 World Ocean Database 2001 Volume 6: Temporal Distribution of pH, Alkalinity, pCO<sub>2</sub> and tCO<sub>2</sub> Data. Levitus, S. (ed.), 235 pp (U.S. Gov. Printing Office, Washington D.C., 2002).
- Key, R. M. et al. A global ocean carbon climatology: Results from GLODAP. *Global Biogeochem. Cycles* **18**, GB4031, doi:10.1029/2004GB002247 (2004).
- McGrath, T., Kivimae, C., Tanhua, T., Cave, R. R. & McGovern, E. Inorganic carbon and pH levels in the Rockall Trough 1991–2010. *Deep-Sea Res. I* **68**, 79–91 (2012).
- Lunden, J. J., Georgian, S. E. & Cordes, E. E. Aragonite saturation states at cold-water coral reefs structured by *Lophelia pertusa* in the northern Gulf of Mexico. *Limnol. Oceanogr.* **58**, 354–362 (2013).
- Flögel, S., Dullo, W.-C., Pfannkuche, O., Kiriakoulakis, K. & Rüggeberg, A. Geochemical and physical constraints for the occurrence of living cold-water corals. *Deep-Sea Res. II* http://dx.doi.org/10.1016/j.dsr2.2013.06.006i (2013).
- McGrath, T., Nolan, G. & McGovern, E. Chemical characteristics of water masses in the Rockall Trough. *Deep-Sea Res. I* **61**, 57–73 (2012).
- Wilson, J. B. 'Patch' development of the deep-water coral *Lophelia pertusa* (L.) on Rockall Bank. *J. Mar. Biol. Ass. U.K.* **59**, 165–177 (1979).
- Roberts, J. M., Long, D., Wilson, J. B., Mortensen, P. B. & Gage, J. D. The cold-water coral *Lophelia pertusa* (Scleractinia) and enigmatic seabed mounds along the north-east Atlantic margin: are they related? *Mar. Poll. Bull.* **46**, 7–20 (2003).



23. van Weering, T. C. E., de Haas, H., de Stigter, H. C., Lykke-Andersen, H. & Kouvaev, I. Structure and development of giant carbonate mounds at the SW and SE Rockall Trough margins, NE Atlantic Ocean. *Mar. Geol.* **198**, 67–81 (2003).
24. Kenyon, N. H., Akhmetzhanov, A. M., Wheeler, A. J., van Weering, T. C. W., de Haas, H. & Ivanov, M. K. Giant carbonate mud mounds in the southern Rockall Trough. *Mar. Geol.* **195**, 5–30 (2003).
25. Roberts, J. M., Wheeler, A. J. & Freiwald, A. Reefs of the deep: the biology and geology of cold-water ecosystems. *Science* **312**, 543–547 (2006).
26. Douarin, M. *et al.* Growth of north-east Atlantic cold-water coral reefs and mounds during the Holocene: a high resolution U series and <sup>14</sup>C chronology. *Earth Planet. Sci. Lett.*, <http://dx.doi.org/10.1016/j.epsl.2013.05.023>, in press (2013).
27. Roberts, J. M., Brown, C. J., Long, D. & Bates, C. R. Acoustic mapping using a multibeam echosounder reveals cold-water coral reefs and surrounding habitats. *Coral Reefs* **24**, 654–669 (2005).
28. Roberts, J. M. *et al.* Mingulay reef complex: an interdisciplinary study of cold-water coral habitat, hydrography and biodiversity. *Mar. Ecol. Prog. Ser.* **397**, 139–151 (2009).
29. Findlay, H. S. *et al.* Tidal downwelling and implications for the carbon biogeochemistry of cold-water corals in relation to future ocean acidification and warming. *Glob. Change Biol.* **19**, 2708–2719, doi: 10.1111/gcb.12256 (2013).
30. Mienis, F. *et al.* Hydrodynamic controls on cold-water coral growth and carbonate-mound development at the SW and SE Rockall Trough Margin, NE Atlantic Ocean. *Deep-Sea Res I* **54**, 1655–1674 (2007).
31. Redfield, A. C. The biological control of chemical factors in the environment. *American Scientist* **46**, 205–221 (1958).
32. McCulloch, M. *et al.* Resilience of cold-water scleractinian corals to ocean acidification: Boron isotopic systematics of pH and saturation state up-regulation. *Geoch. et Cosmochim. Acta* **87**, pp. 21–34 (2012).
33. Jantzen, C., Häussermann, V., Försterra, G., Laudien, J., Ardelan, M., Maier, S. & Richter, C. Occurrence of cold-water coral along natural pH gradients (Patagonia, Chile). *Mar. Biol.* **160**, 2597–2607, doi: 10.1007/s00227-013-2254-0 (2013).
34. Carilli, J., Donner, S. D. & Hartmann, A. C. Historical Temperature Variability Affects Coral Response to Heat Stress. *PLoS ONE* **7**, e34418, doi:10.1371/journal.pone.0034418 (2012).
35. Maier, C., Schubert, A., Berzunza Sánchez, M. M., Weinbauer, M. G., Watremez, P. & Gattuso, J.-P. End of century pCO<sub>2</sub> levels do not impact calcification in Mediterranean cold-water corals. *PLoS ONE* **8**, e62655, doi:10.1371/journal.pone.0062655 (2013).
36. Maier, C., Bils, F., Weinbauer, M. G., Watremez, P., Peck, M. A. & Gattuso, J.-P. Respiration of Mediterranean cold-water corals is not affected by ocean acidification as projected for the end of the century. *Biogeosci.* **10**, 5671–5680, doi:10.5194/bg-10-5671-2013 (2013).
37. McCulloch, M., Falter, J., Trotter, J. & Montagna, P. Coral resilience to ocean acidification and global warming through pH up-regulation. *Nature Climate Change* **2**, 623–627, DOI: 10.1038/NCLIMATE1473 (2012).
38. Orr, J. *et al.* Anthropogenic ocean acidification over the twenty-first century and its impact on calcifying organisms. *Nature* **437**, 681–686 (2005).
39. Form, A. U. & Riebesell, U. Acclimation to ocean acidification during long-term CO<sub>2</sub> exposure in the cold-water coral *Lophelia pertusa*. *Global Change Biol.* **18**, 843–853, doi: 10.1111/j.1365-2486.2011.02583.x (2012).
40. Hennige, S. J. *et al.* Short-term metabolic and growth responses of the cold-water coral *Lophelia pertusa* to ocean acidification. *Deep-Sea Res. II* <http://dx.doi.org/10.1016/j.dsr2.2013.07.005> (2013).
41. Henry, L.-A. & Roberts, J. M. Biodiversity and ecological composition of macrobenthos on cold-water coral mounds and adjacent off-mound habitat in the bathyal Porcupine Seabight, NE Atlantic. *Deep-Sea Res. I* **54**, 654–672 (2007).
42. Wisshak, M., Schönberg, C. H. L., Form, A. & Freiwald, A. Ocean acidification accelerates reef bioerosion. *PLoS ONE* **7**, e45124, doi:10.1371/journal.pone.0045124 (2012).
43. Ramirez-Llodra, E., Tyler, P. A., Baker, M. C., Aksel Bergstad, O., Clark, M. R., Escobar, E., Levin, L. A., Menot, L., Rowden, A. A., Smith, C. R. & Van Dover, C. L. Man and the last great wilderness: Human impact on the deep sea. *PLoS ONE* **6**, e22588, doi:10.1371/journal.pone.0022588 (2011).
44. Findlay, H. S. CTD data from James Cook Research Cruise JC073. British Oceanographic Data Centre - Natural Environment Research Council, UK. doi:10/nvv (2013).
45. Findlay, H. S. & Woodward, E. M. S. Carbon and nutrients concentrations associated with RRS James Cook cruise JC073. British Oceanographic Data Centre - Natural Environment Research Council, UK. doi:10/nvt. (2013).
46. Roberts, J. M. & shipboard party. Changing Oceans Expedition 2012. *RRS James Cook 073 Cruise Report* (Heriot-Watt University, Edinburgh, (2013).
47. Behrenfeld, M. J. & Boss, E. The beam attenuation to chlorophyll ratio: an optical index of phytoplankton physiology in the surface ocean? *Deep-Sea Res. I*, **50**, 1537–1549 (2003).
48. Grasshoff, K. Methods of seawater analysis. *Verlag chemie*, pp. 317. (Weinheim, 1976).
49. Schlitzer, R. Ocean Data View. <http://odv.awi.de> (2013).
50. Dickson, A. G., Sabine, C. L. & Christian, J. R. Guide to Best Practices for Ocean CO<sub>2</sub> Measurements. *PICES special publication* **3**, IOCC Report No. 8 (2007).
51. Woodward, E. M. S. & Rees, A. P. Nutrient distributions in an anticyclonic eddy in the North East Atlantic Ocean, with reference to nanomolar ammonium concentrations. *Deep-Sea Res. II* **48**, 775–794 (2001).
52. Brewer, P. G. & Riley, J. P. The automatic determination of nitrate in sea water. *Deep-Sea Res.* **12**, 765–772 (1965).
53. Zhang, J. & Chi, J. Automated analysis of nanomolar concentrations of phosphate in natural waters with liquid waveguide. *Environ. Sci. Tech.* **36**, 1048–1053 (2002).
54. Kirkwood, D. S. Simultaneous determination of selected nutrients in sea water. *Int. Council Expl. Sea* **1989/C:29** (1989).
55. Pierrot, D., Lewis, E. & Wallace, D. W. R. CO<sub>2</sub>sys DOS program developed for CO<sub>2</sub> system calculations. ORNL/CDIAC-105, (Carbon Dioxide Information Analysis Center, Oak Ridge National Laboratory, U.S. Department of Energy, Oak Ridge, Tennessee, 2006).
56. Mehrbach, C., Culbertson, C. H., Hawley, J. E. & Pytkowicz, R. M. Measurements of the apparent dissociation constants of carbonic acid in seawater at atmospheric pressure. *Limnol. Oceanogr.* **18**, 897–907 (1973).
57. Dickson, A. G. & Millero, F. J. A comparison of the equilibrium constants for the dissociation of carbonic-acid in seawater media. *Deep-Sea Res.* **34**, 1733–1743 (1987).
58. Dickson, A. G. Thermodynamics of the dissociation of boric acid in potassium-chloride solutions from 273.15 K to 318.15 K. *J. Chem. Thermodyn.* **22**, 113–127 (1990).
59. Friis, K., Körtzinger, A. & Wallace, D. W. R. The salinity normalization of marine inorganic carbon chemistry data. *Geophys. Res. Lett.* **30**, 2, 1085, doi:10.1029/2002GL015898 (2003).
60. Anderson, M. J., Gorley, R. N. & Clarke, K. R. *PERMANOVA+ for PRIMAER: Guide to software and statistical methods*. (PRIMER-E Ltd, Plymouth, 2008).

## Acknowledgments

This work was carried out as part of the UK Ocean Acidification Research Programme's Benthic Consortium project (awards NE/H01747X/1 and NE/H017305/1) funded by NERC, Defra and DECC. S.J.H., J.M.N., J.M.R. and L.W. acknowledge additional support from Heriot-Watt University's Environment & Climate Change theme. The authors would also like to thank the Captain, crew and technicians aboard the RRS *James Cook* (cruise JC073); special thanks go to Lissette Victorero Gonzalez for laboratory assistance and Karl Attard for carrying out oxygen Winkler Titrations. All data from cruise JC073 have been deposited at the British Oceanographic Data Centre (BODC).

## Author contributions

H.S.F., S.J.H., L.C.W. and J.M.N. collected the data. H.S.F. and E.M.S.W. analyzed the data. H.S.F. wrote the paper, and all authors (H.S.F., S.J.H., J.M.N., L.C.W., E.M.S.W. and J.M.R.) contributed to the final text and figures.

## Additional information

**Supplementary information** accompanies this paper at <http://www.nature.com/scientificreports>

**Competing financial interests:** The authors declare no competing financial interests.

**How to cite this article:** Findlay, H. S. *et al.* Fine-scale nutrient and carbonate system dynamics around cold-water coral reefs in the northeast Atlantic. *Sci. Rep.* **4**, 3671; DOI:10.1038/srep03671 (2014).



This work is licensed under a Creative Commons Attribution 3.0 Unported license. To view a copy of this license, visit <http://creativecommons.org/licenses/by/3.0>